TUDelft

Delft University of Technology

Optimum Layouts of a Cluster of Heaving Point Absorbers in front of a Wall

Loukogeorgaki, Eva; Michailides, Constantine ; Lavidas, G.; Chatjigeorgiou, Ioannis K.

Citation (APA)
Loukogeorgaki, E., Michailides, C., Lavidas, G., & Chatjigeorgiou, I. K. (2021). Optimum Layouts of a Cluster of Heaving Point Absorbers in front of a Wall. In *The Thirty-first (2021) International Ocean and Polar Engineering Conference (ISOPE 2021)* (pp. 736-743). International Society of Offshore and Polar Engineers (ISOPE).

Important note
To cite this publication, please use the final published version (if applicable).
Please check the document version above.

Optimum Layouts of a Cluster of Heaving Point Absorbers in front of a Wall

Eva Loukogeorgaki[1], Constantine Michailides[2], George Lavidas[3] and Ioannis K. Chatjigeorgiou[4]
[1]Department of Civil Engineering, Aristotle University of Thessaloniki
Thessaloniki, Greece
[2]Department of Civil Engineering and Geomatics, Cyprus University of Technology
Limassol, Cyprus
[3]Faculty of Civil Engineering and Geosciences, Department of Hydraulic Engineering, Delft University of Technology
Delft, The Netherlands
[4]School of Naval Architecture and Marine Engineering, National Technical University of Athens
Athens, Greece

ABSTRACT

In this paper, we determine optimum layouts of a cluster of oblate spheroidal heaving point absorbers in front of a wall, that maximize the annual averaged power absorbed by the cluster, while satisfying specific spatial constraints. An iterative optimization process is developed by coupling a hydrodynamic model with a genetic algorithms solver. Optimization is performed for three near-shore sites in the Aegean Sea, Greece. Optimum layouts are obtained considering part of or the whole wall length, available for the PAs' sitting. The effect of the incident wave direction on the optimum layouts' formation and the absorbed power is also assessed. Finally, the dependence of the maximized absorbed power upon the deployment site is illustrated.

KEY WORDS: Wave energy; point absorbers; clusters; wall; layout; optimization; genetic algorithms.

INTRODUCTION

Contemporary technological advances seek the efficient exploitation of the vast wave energy potential. Accordingly, the technology of Wave Energy Converters (WECs) is continuously being developed during the past years, aiming at delivering commercially competitive solutions that maximize efficiency, ensure survivability, reduce costs and minimize environmental impacts. Heaving type Point Absorbers (PAs) correspond to one of the most technologically advanced type of WECs, characterized by the "one-mode" operation simplicity. Some characteristic examples of PAs are the Wavestar (Hansen et al., 2013) and the Seabased AB (Chatzigiannakou et al., 2017). In order to absorb an adequate amount of power and, thus, contribute to the reduction of the high Levelized Cost of Electricity (LCoE), representing currently one of the main drawbacks of WECs (Rusu and Onea, 2018), multiple

PAs in the form of clusters (arrays) can be deployed (e.g., Stratigaki et al., 2014; Balitsky et al., 2018).

Alternatively to offshore marine areas, PAs clusters can be also deployed at near-shore locations. In those cases, coastal structures, such as vertical (wall-type) breakwaters, occupying a large ocean space, may exist, while the relevant asset owners and operators may seek for additional integrated alternative uses of the existing marine facilities. Within this context, clusters of PAs can be deployed in the seaward side of wall-type breakwaters facilitating the exploitation of both the incident waves and the waves reflected from the wall. This idea falls within the wider approach of integrating WEC technologies with coastal structures (e.g., Zhao et al., 2019; Rosa-Santos et al., 2019; Vicinanza et al., 2012; Michailides and Angelides, 2015) and it can support the realization of cost-efficient solutions through costs sharing.

The performance (hydrodynamic behavior and power absorption) of a linear array of five cylindrical heaving PAs in front of a bottom-mounted wall has been investigated in the frequency domain by Mavrakos et al. (2004), by utilizing the method of images and, thus, assuming a leeward boundary of infinite length. The same method was deployed by Konispoliatis and Mavrakos (2020) and Konispoliatis et al. (2020), for a linear, parallel or perpendicular to the wall, array as well as for a rectangular cluster of five heaving PAs having vertical axisymmetric floaters (e.g., cylindrical, conical). On the other hand, Loukogeorgaki and Chatjigeorgiou (2019) and Loukogeorgaki et al. (2020) considered the existence of a finite-length bottom-mounted leeward wall for assessing the performance of a cluster of nine cylindrical and five oblate spheroidal, respectively, heaving PAs. In all the above studies, the PAs cluster consisted of equally-spaced devices situated at predefined locations with respect to the wall. Furthermore, in most of these investigations, the dependence of the cluster's power

absorption ability upon the locations of the PAs with respect to the wall and within the cluster was highlighted. Hence, optimizing the layout of a PAs cluster can be considered as a key issue towards the efficient deployment of heaving PAs in front of wall-type coastal structures. So far, the significance of optimizing the layout of WECs has been extensively demonstrated in the case of isolated (i.e., without the wall presence) clusters (e.g. Göteman et al., 2020) by developing and applying either traditional evolutionary optimization algorithms (e.g., Child and Venugopal, 2010; Ruiz et al., 2017; Sharp and DuPont, 2018) or other advanced approaches, such as the machine learning approach (Sarkar et al., 2016) and the artificial neural networks (Neshat et al., 2019).

In this paper, we develop an optimization process to determine the optimum layout of a cluster of PAs in front of a bottom-mounted vertical wall of finite length under the action of long-crested irregular waves. The term "optimum" refers to layouts that maximize the annual power absorbed by the cluster and satisfy predefined spatial constraints. The proposed optimization process is numerically realized by coupling appropriately a frequency-based hydrodynamic model, which solves the diffraction/radiation problem of the multi-body arrangement in the presence of the wall, with a Genetic Algorithms (GAs) optimization solver. Optimization is performed for a cluster of five, identical, oblate spheroidal PAs deployed at three different near-shore sites in the Aegean Sea, Greece. The required wave climate matrices are acquired by a numerical wave model, specifically developed for the Aegean Sea. Optimum layouts are, initially, obtained for perpendicular to the wall waves, considering either part of the wall length or the whole wall length, available for the placement of the PAs. Finally, the effect of oblique waves on the formation of the optimum layouts and on the power absorbed by the cluster is examined.

FORMULATION OF THE OPTIMIZATION PROBLEM

We consider a cluster of Q hydrodynamically interacting semi-immersed heaving PAs in front of bottom-mounted, vertical wall at a marine site of water depth d (Fig. 1). The wall has finite length l_{wall}, while its thickness is assumed negligible. The cluster consists of identical PAs having an oblate spheroidal shape of equatorial radius (semi-major axis) and polar radius (semi-minor axis) a and b respectively (Fig. 1b). Each PAq, $q=1,…, Q$, is assumed to absorb power through a linear PTO mechanism, which is actuated by the device's forced motion in heave and is schematically represented in Fig. 1b as a linear damping system of damping coefficient b_{PTOq}. The PAs are spatially distributed within the cluster, with the X, Y coordinates of the centers of the PAs in the global $OXYZ$ coordinate system, X_q and Y_q, $q=1,…, Q$, respectively (Fig. 1a), denoting the unknown locations of the devices in the seaward side of the wall. The marine site, where the arrangement is situated, is characterized by its local wave climate; namely, a set of sea states, each of which is described by a wave spectrum of significant wave height H_s and peak period T_p and has an annual probability of occurrence $Pr (H_s, T_s)$.

Considering all the above, we aim to determine the optimum layout of the PAs in front of the wall or, equivalently. the optimum values of the coordinates X_q and Y_q, $q=1,…, Q$, that lead to the maximization of the annual averaged power absorbed by the whole cluster, p_{annual}, at a given marine site, while satisfying specific spatial constraints. Accordingly, by defining X_q and Y_q, $q=1,…, Q$, as the design variables and p_{annual} as the objective function to be maximized, the examined in this paper constrained optimization problem, takes the form:

$$\text{maximize } p_{annual}\left(X_1,...,X_q,...,X_Q,Y_1,...,Y_q,...,Y_Q\right) \quad (1)$$

where:

$$p_{annual} = \left(\sum_{H_s}\sum_{T_p} Pr\left(H_s,T_p\right)p\left(H_s,T_p\right)\right) \quad (2)$$

subjected to:

$$\sqrt{\left(X_q - X_l\right)^2 + \left(Y_q - Y_l\right)^2} > 2a \text{ for } q,l = 1,...,Q \text{ and } q \neq l \quad (3)$$

$$1.1a \leq Y_q \leq 3a \text{ for } q = 1,...,Q \quad (4)$$

For odd Q number $\begin{cases} X_q = -X_{Q+1-q} & \text{for } q = 1,...,(Q/2-0.5) \\ X_{Q/2+0.5} = 0 \\ Y_q = Y_{Q+1-q} & \text{for } q = 1,...,(Q/2-0.5) \end{cases}$ (5a)

or

For even Q number $\begin{cases} X_q = -X_{Q+1-q} & \text{for } q = 1,...,Q/2 \\ Y_q = Y_{Q+1-q} & \text{for } q = 1,...,Q/2 \end{cases}$ (5b)

$$\left|X_q\right| \leq \left(\frac{l_{wall}}{2} - l_{edge}\right) \text{ for } q = 1 \text{ and } Q \quad (6)$$

$$X_q \in \left[-\frac{l_{wall}}{2},\frac{l_{wall}}{2}\right] \text{ for } q = 1,...,Q \quad (7)$$
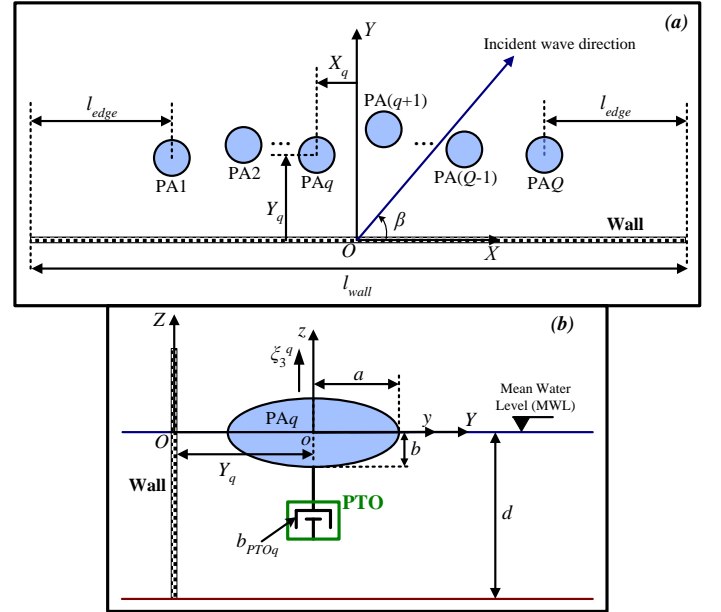

Fig. 1 Geometry of the examined cluster-wall arrangement: (a) X-Y plane, (b) Y-Z plane

In Eq. 2, $p(H_s, T_p)$ is the averaged power absorbed by the cluster for a given sea state of H_s and T_p, as defined in the next section, and l_{edge} denotes parts of l_{wall} close to the wall's two ends, where the PAs cannot be deployed (Fig. 1a). Regarding the spatial constraints, Eq. 3 expresses mathematically the avoidance of overlapping between any two PAs within the cluster, whereas Eq. 4 imposes spatial restrictions

on the perpendicular distances of the devices from the wall. More specifically, the lower bound of Eq. 4, equal to $1.1a$, ensures avoidance of overlapping between the PAs and the wall, while the upper bound of this equation ensures placement of the devices within a maximum distance from the leeward boundary. The value of this upper bound has been defined based on Loukogeorgaki et al. (2020), who demonstrated reduced power absorption ability of a linear array of oblate spheroidal PAs, when the array is deployed at a distance from the wall larger than $3a$. Continuing with the rest spatial constraints, Eqs. 5a~5b facilitate the realization of symmetrical layouts with respect to the global OY axis, while Eq. 6 expresses mathematically the utilization of part of the total available wall length l_{wall} for placing the PAs cluster. Finally, Eq. 7 ensures the placement of all the devices in front of the wall within its two ends.

SOLUTION OF THE OPTIMIZATION PROBLEM

In order to solve the constrained optimization problem described above, an iterative optimization process is developed and applied by coupling appropriately within MATLAB (MATLAB, 2019) a frequency-based hydrodynamic model with a GAs optimization solver. This process is shown schematically in Fig. 2, while in the following sub-sections details about the hydrodynamic model and its coupling with the GAs solver are provided.
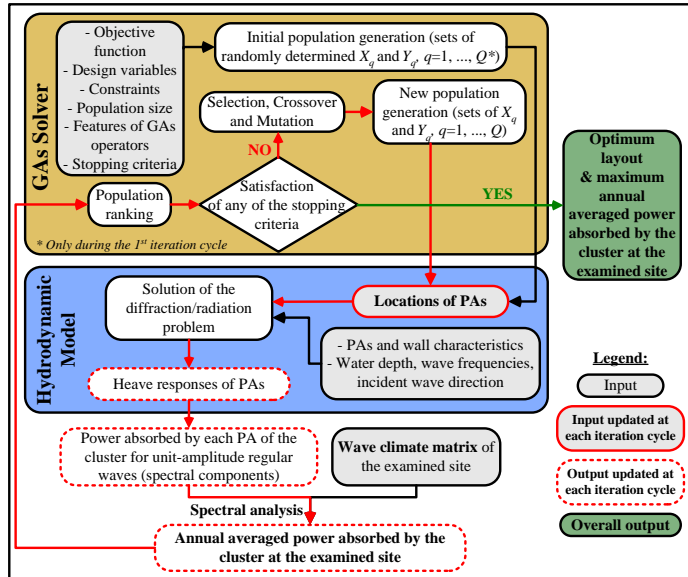

Fig. 2 Flow chart of the optimization process developed and applied in the present investigation

Frequency-based Hydrodynamic Model

The hydrodynamic analysis of the PAs cluster in front of the bottom-mounted wall under the action of regular waves, including the hydrodynamic interaction effects among the PAs and between the wall and the devices, is implemented in the frequency domain and it is based on the boundary integral equation method. This method is numerically realized using WAMIT software (Lee, 1995) and it is considered high suitable for assessing the power absorption ability of small WECs clusters, consisting of 2-10 devices (Folley et al., 2012). A three-dimensional linear potential theory is utilized, where, the wall is considered fixed at its position, while a q-th PA, is taken to undergo small amplitude oscillations of complex amplitude ξ_3^q, $q=1,\ldots,Q$, only along its working direction, i.e., along its local vertical axis (Fig.

1b). Thus, all degrees of freedom of the PAs except the one corresponding to heave, are regarded ideally restricted. It is noted that pure heaving devices can be physically realized by appropriately attaching the PAs on the wall, as, for example, in the case of a hybrid wind–wave monopile support structure (Gkaraklova et al., 2021). The fluid is assumed inviscid and incompressible, while the flow is assumed irrotational. Hence, the fluid motion is described in terms of the velocity potential, which satisfies the Laplace equation. Its complex spatial part is defined as (Lee, 1995; Lee and Newman, 2005):

$$\varphi = \underbrace{\varphi_I + \varphi_S}_{\varphi_D} + i\omega \sum_{q=1}^{Q} \xi_3^q \varphi_q \tag{8}$$

$$\varphi_I = \frac{igA}{\omega} \frac{\cosh\left[k(Z+d)\right]}{\cosh(kd)} e^{-ik(X\cos\beta + Y\sin\beta)} \tag{9}$$

where φ_I, φ_S, φ_D and φ_q, $q=1,\ldots,Q$, are, respectively, the incident, scattered, diffracted and unit-amplitude radiation (in heave) potentials, ω and A are the frequency and the amplitude of the incident waves, that propagate at an angle β relative to the OX axis (Fig. 1a), g is the gravitational acceleration, k is the wave number and $i^2=-1$. The potential φ_S is associated with the disturbances of the incident waves induced by the PAs and the wall fixed at their positions, while the potentials φ_q, $q=1,\ldots,Q$, are related to the waves radiated from the PAs due to their unit-amplitude forced motion in heave.

In order to form the first order boundary value problem, the potentials are subjected to appropriate linearized boundary conditions, corresponding to the combined kinematic and dynamic free-surface condition, the bottom boundary condition and the Neumann boundary conditions on the wetted surface of the bodies (Lee, 1995; Lee and Newman, 2005). The boundary integral equations for the unknown diffraction and unit-amplitude radiation potentials on the boundary of the PAs and the wall, and of the PAs respectively are, then, formulated by utilizing Green's theorem, and the boundary value problem is, finally, solved based on a three dimensional low-order panel method (Lee, 1995; Lee and Newman, 2005). The assumption of a wall of negligible thickness leads to the deployment of zero-thickness dipole panels (Lee and Newman, 2005) in order to model its wetted surface. Subsequently, the heave exciting forces, F_3^q, as well as the heave added mass and radiation damping coefficients, A_{ql} and B_{ql}, q, $l=1,\ldots,Q$, respectively, are calculated using Eqs. 10~11, where n_3^q is the unit normal vector on the wetted surface S_{Bq} of the q-th PA in the vertical direction and ρ is the seawater density:

$$F_3^q = -i\omega\rho \iint_{S_{Bq}} n_3^q \varphi_D ds, \quad q=1,\ldots,Q \tag{10}$$

$$A_{ql} - \frac{i}{\omega}B_{ql} = \rho \iint_{S_{Bq}} n_3^q \varphi_l ds, \quad q, l=1,\ldots,Q \tag{11}$$

The complex amplitudes of the PAs' motions, ξ_3^q, $q=1,\ldots,Q$, are, then, obtained from the solution of the following linear system of equations:

$$\sum_{q=1}^{Q}\left[-\omega^2(M_{ql}+A_{ql})+i\omega(B_{ql}+B_{ql}^{PTO})+C_{ql}\right]\xi_3^q = F_3^l, \quad l=1,\ldots,Q \tag{12}$$

where M_{ql} and C_{ql} are respectively the mass matrix and the hydrostatic-gravitational stiffness coefficients and B_{ql}^{PTO} are the damping coefficients originating from the PAs' PTO mechanism. For a q-th PA, the latter mechanism is modeled as a linear damping system with damping coefficient b_{PTOq}. Hence, in Eq. 12, $B_{ql}^{PTO} = b_{PTOq}$ for $q=l=1,\ldots, Q$, while, $B_{ql}^{PTO} = 0$ for $q \neq l$.

The averaged power, $p_q(\omega)$, absorbed by a q-th PA of the cluster under the action of unit-amplitude regular incident waves of frequency ω results from Eq. 13, where $\left| \xi_3^q \right|$ is the amplitude of the complex quantity ξ_3^q :

$$p_q(\omega) = \frac{1}{2} b_{PTOq} \omega^2 \left| \xi_3^q \right|^2 \qquad (13)$$

Having obtained $p_q(\omega)$ for various values of ω representing the frequency components of a spectrum, a spectral analysis follows by deploying the wave climate matrix at the marine site, where the multi-body arrangement is taken to be situated (Fig. 2). This analysis aims at calculating the annual averaged power absorbed by the cluster, p_{annual}, at the examined site, and, thus, quantifying the objective function of the optimization problem (Eqs. 1~2). Specifically, for each sea state described by a spectrum of H_s and T_p, the averaged power absorbed by the whole cluster $p(H_s, T_p)$ is obtained as follows:

$$p(H_s, T_p) = \sum_{q=1}^{Q} p_q(H_s, T_p) = \sum_{q=1}^{Q} \int_0^\infty S(\omega \,|\, H_s, T_p) p_q(\omega) d\omega \qquad (14)$$

In Eq. 14, $p_q(H_s, T_p)$, $q=1,\ldots, Q,$ is the power absorbed by the q-th PA for the given sea state, $S(\omega \,|\, H_s, T_p)$ is the spectral density of the spectrum taken into account, whereas the symbol "|" denotes given values of H_s and T_p. Eq. 14 is applied for all the sea states forming the wave climate matrix at the examined site. For each sea state, $p(H_s, T_p)$ is, then, multiplied by the corresponding annual probability of occurrence, $Pr(H_s, T_s)$, and the results are summed up in order to obtain p_{annual} (Eq. 2).

Coupling of the Hydrodynamic Model with the GAs Optimization Solver

The hydrodynamic model described above is appropriately coupled with a GAs optimization solver in order to implement numerically the optimization process of Fig. 2. The deployed GAs solver corresponds to an evolutionary algorithm that mimics the process of natural evolution according to the "survival of the fittest" rule by employing relevant computational operators (Deb, 2001). The efficiency of GAs for solving optimization problems related to isolated WECs clusters has been already demonstrated in Child and Venugopal (2010) and Ruiz et al. (2017). The solver is numerically realized by using the Optimization Toolbox™ R2019b of MATLAB (MATLAB, 2019). For the optimization process considered herein, an individual of a population, which represents a candidate solution, corresponds to a specific set of values of the design variables, X_q and Y_q, $q=1,\ldots, Q$. The size of the population, which is equal to the number of the individuals, remains constant during the execution of the GAs solver, while, furthermore Eqs. 3~7 are taken into account, when individuals are generated, so that

the constraints and the bounds for the design variables are always satisfied.

Initially (Fig. 2), the objective function (Eqs. 1~2), the design variables X_q and Y_q, $q=1,\ldots, Q$, the constraints (Eqs. 3~7), the size of the populations, the features of the GAs operators and the stopping criteria are provided as input to the GAs solver. The computational evolution starts with the generation of an initial constraint-dependent random population. The individuals of this population are used as input to the hydrodynamic model along with the values of the rest physical quantities required for executing this model (Fig. 2). The corresponding diffraction/radiation problem is, then, solved for each individual and the PAs' heave responses are obtained (Eq. 12). Accordingly, the averaged power absorbed by each PA of the cluster under the action of unit-amplitude regular waves representing the components of a wave spectrum is calculated (Eq. 13) and, finally, by deploying Eq. 14 and Eq. 2 for the wave climate matrix of the examined site, the objective function, p_{annual}, is quantified. Based on the values of p_{annual}, the individuals of the initial population are, then, ranked in descending order and the stopping criteria are checked. If any of these criteria is not satisfied, a new population of individuals is generated by deploying the selection, the mutation and the crossover operators. Specifically, an upper percentage of the ranked individuals is selected to survive and continue to the next generation. Among these individuals, the highest ranked ones are selected as "elite" and, thus, they are maintained within the next population without any change, whereas, the rest individuals are selected as "parents" and, hence, they are deployed for the generation of new individuals (selection operator). The latter generation is realized by: (a) combining the design variables entries of a pair of "parents" to generate a fitter offspring (crossover operator) and (b) changing randomly the entries of a single "parent" so as to maintain diversity within the population (mutation operator). The individuals of the new population are used as input in the hydrodynamic model to calculate new values of the PAs' heave responses and, thus, new values of p_{annual}. These individuals are, then, ranked and the stopping criteria are again checked. Having satisfied one of the stopping criteria, the individual of the last generated population with the highest ranking is assigned as the optimum solution of the constrained maximization problem examined. Details about the GAs characteristics (e.g. population size, type of stopping criteria, etc.) utilized in the present paper are cited in the next section.

INVESTIGATED CASES

A cluster of $Q=5$ identical oblate spheroidal PAs (Fig. 1a with $Q=5$) in front of a wall of total non-dimensional length $l_{wall}/a=36$ is considered to be deployed at three different marine sites. Those sites correspond to near-shore locations at Siros (Site S1), Anafi (Site S2) and Karpathos (Site S3) islands in the Aegean Sea, Greece (Fig. 3) and are characterized by good capacity factors and high accessibility for near-shore heaving PAs (Lavidas and Venugopal, 2017; Lavidas et al., 2018).

Based on Tzellos et al. (2020), each q-th PA within the cluster is selected to have equatorial radius $a=2.0$ m, non-dimensional polar radius $b/a=0.85$ and a constant damping coefficient b_{PTO} (i.e., in Eq. 12, $b_{PTOq}=b_{PTO}$ for $q=1,\ldots, 5$). This coefficient is appropriately tuned, so that the energy absorption of the PA is maximized at the natural frequency, ω_{n3}, of a single, isolated device. Thus, and in line with Falnes and Kurniawan (2020), b_{PTO} is taken equal to $B_{33}(\omega=\omega_{n3})$, where B_{33} is the heave radiation damping of a single, isolated PA. For the examined geometry, ω_{n3} is 2.4 rad/s (the corresponding natural period in heave, T_{n3}, is 2.6 s) leading to $b_{PTO}=10.322$ kNs/m (Loukogeorgaki et al., 2020).

For each examined site, three different optimization cases have been considered and solved. In the first case (OPC1), Eq. 6 is applied for a non-dimensional l_{edge}/a value equal to 10; thus, a non-dimensional wall length of 16 is only considered available for the placement of the PAs cluster. Contrary to OPC1, the second optimization case (OPC2) considers the whole wall length available for the PAs' placement. This physical consideration is numerically realized by setting l_{edge}=0 m in Eq. 6. In both OPC1 and OPC2, perpendicular to the wall waves are taken into account (i.e. β=270º, Fig. 1a). Finally, the third optimization case (OPC3) is similar with OPC2; however, the action of waves with β=247.5º (Fig. 1a) is considered, so that the effect of oblique waves on the annual power absorbed by the cluster and on the formation of the optimum cluster layouts can be demonstrated.
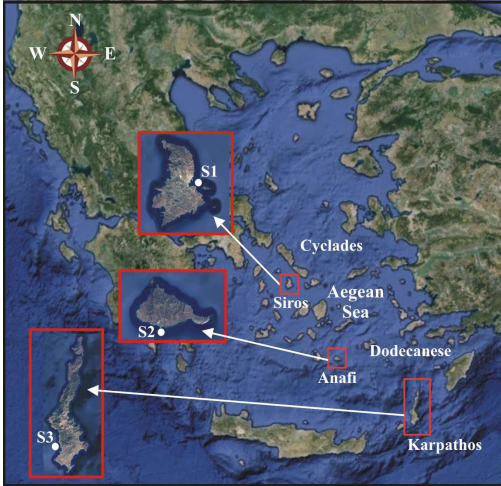

Fig. 3 Locations of examined sites

The hydrodynamic analysis has been performed for non-dimensional water depth d/a equal to 3.5, 4 and 5 for S1, S2 and S3 respectively and for unit-amplitude regular waves with ω varying between 0.05 rad/s and 4.0 rad/s. These values also represent the cut-off spectral frequencies deployed in Eq. (14), which, in the present paper, is applied by utilizing the TMA spectrum (e.g., Hughes, 1984; Bergdahl, 2009). The latter spectrum has a finite depth spectral formulation and corresponds to a modified Jonswap spectrum in shallow waters. Accordingly, it enables the consideration of limited water depth conditions. For a given sea state with H_s and T_p, $S(\omega \mid H_s, T_p)$ for the TMA spectrum can be obtained by multiplying the corresponding spectral density of the Jonswap spectrum with the so-called "limited depth" function, $\Phi(d,\omega)$, given by Eq. 15 below (e.g., Bergdahl 2009). The spectral density of the Jonswap spectrum was obtained using the well-known relevant formulation (e.g., DNV-GL, 2017).

$$\Phi(d,\omega) = \begin{cases} 0.5\left(\omega\sqrt{d/g}\right)^2 & \text{for } \omega\sqrt{d/g} < 1 \\ 1.0 - 0.5\left(2 - \omega\sqrt{d/g}\right)^2 & \text{for } 1 \leq \omega\sqrt{d/g} < 2 \\ 1.0 & \text{for } \omega\sqrt{d/g} \geq 2 \end{cases} \quad (15)$$

The wave climate matrices of the three examined sites were acquired by a hind-cast, based on the spectral phased averaged model Simulating WAves Nearshore (SWAN), specifically developed for the Aegean Sea (Lavidas and Venugopal, 2017). The model utilized a two way nesting for the Mediterranean and the Aegean Seas and provided a

comprehensive resource assessment of metocean conditions for 35 years from 1980 to 2014, after being appropriately calibrated. Based on the spatial resolution of the aforementioned model, the 35-years H_s and T_p data for S1, S2 and S3 were obtained at a water depth equal to 11.5 m, 18.7 m and 27.0 m, respectively. For all locations, non-linear wave interactions have been considered in the application of SWAN.

Finally, for the GAs solver the following options have been defined at the beginning of the analysis: (a) design variables (X_q and Y_q, q=1,…, 5) with values up to their first decimal (i.e., consideration of 0.1 m X 0.1 m grid), (b) population size equal to 10 with double-precision variables, (c) adaptive feasible mutation, (d) 0.6 crossover fraction, (e) 2 individuals as "elites" and, thus, 8 individuals for generation. The process was terminated if the change in the fitness function (p_{annual}) value over 8 generations was less than 0.01 (stopping criterion). For the optimization problems solved, 11 iterations were required at an average to achieve convergence, while the average computational time for one iteration (10 runs of the hydrodynamic model) was approximately equal to 3 minutes using a standard PC with 128 GB RAM and Intel® Xeon® Silver 4110 CPU@ 2.1 GHz 2.1 GHz (2 processors).

RESULTS AND DISCUSSION

Starting with the local wave climate at the three examined sites, Fig, 4 shows, in the form of contours, the annual probability of occurrence, $Pr(H_s,T_p)$, of the various sea states in percentage (%). It can be seen that sea states of significant wave height up to 1.75 m (site S1) or up to 2.25 m (sites S2 and S3) show the largest probability of occurrence; thus, all sites are characterized by a mild wave environment. Furthermore, for sites S1 and S2 (Figs. 4a~4b) located in the Central Aegean, sea states with large probability of occurrence have $3.0 \text{ s} \leq T_p \leq 6.0 \text{ s}$ and $4.0 \text{ s} \leq T_p \leq 6.0 \text{ s}$, respectively. However, for site S3 located in South-Eastern Aegean (Fig. 4c), the most frequent sea states are distributed within a bit wider T_p range, i.e., at $4.0 \text{ s} \leq T_p < 7.0 \text{ s}$.
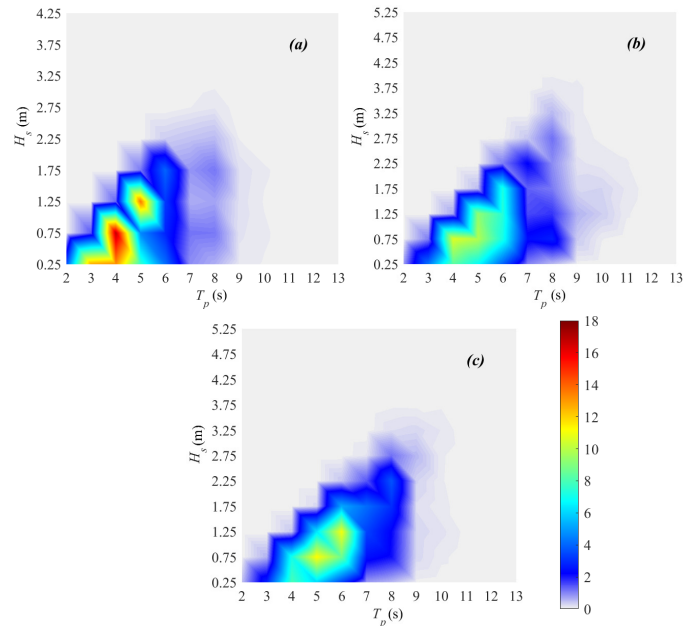

Fig. 4 $Pr(H_s,T_p)$ (%) for sites S1 (a), S2 (b) and S3 (c)

Continuing with the optimization results, Fig. 5 shows schematically the optimum layouts of the PAs cluster in front of the wall in the *X-Y*

plane for the first examined optimization case (OPC1), where the PAs are constrained to be situated along part of the available wall length (i.e., at $-8.0 \leq X/a \leq 8.0$). For all three sites, optimum layouts are realized by placing all the PAs along a straight, parallel to the wall, line at Y/a=1.1. It is recalled that the heave natural period of the examined device, T_{n3}, is equal to 2.6 s and, thus, it is smaller compared to the T_p values of the most frequent sea states. For these specific characteristics, the optimum value of Y/a=1.1 advocates that positive hydrodynamic interactions between the PAs and the wall in terms of power absorption occur, when the devices are situated at the smallest allowable perpendicular distance from the leeward boundary. This conclusion agrees with the parametric results obtained by Loukogeorgaki et al. (2020) for a linear array of five oblate spheroidal PAs with b/a=0.85 under the action of regular waves.

Regarding the distribution of the PAs within the optimum cluster layouts, for all three sites, the middle PA (PA3) is located at X_3/a=0, due to symmetrical considerations (Eq. 5a), while the two outer devices (PA1 and PA5) are located at the two edges of the available wall length (i.e., at X_1/a=-8 and X_5/a=8 respectively). In the case of sites S2 and S3, the remaining two PAs (PA2 and PA4) are situated close to the middle one; thus, a sub-cluster of closely-positioned devices in the middle part of the wall is formed. This is not observed for site S1, where the optimum values of X_2/a=-3.95 and X_4/a=3.95 lead to an almost uniform distribution of the PAs within the available wall length.
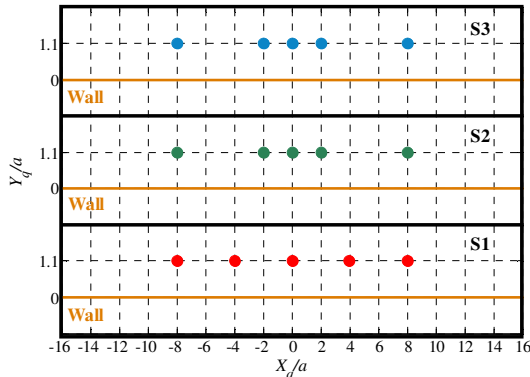
Fig. 5 Optimum layouts of the PAs cluster in front of the wall for S1~S3 and for OPC1
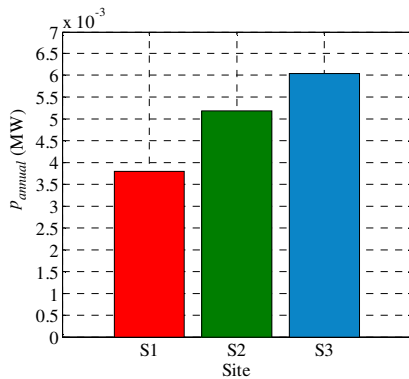
Fig. 6 p_{annual} for S1~S3 for the optimally-arranged clusters of OPC1

As for the annual power absorbed by the optimally-arranged PAs (Fig. 6), the largest p_{annual} value among all examined sites equal to 6.05 kW, is obtained in the case of S3, while for sites S2 and S1 the power

absorption ability of the corresponding optimum layouts is reduced by 14.2% and 37.1%, respectively compared to S3. For sites S2 and S3 similar local wave climates exist (Figs. 4b~4c) and same optimum cluster layouts have been obtained (Fig. 5). However, the deployment of the PAs cluster at d/a=4 in the case of S2 contrary to d/a=5 considered for S3, reduces the finite-depth spectral densities of the incident wave spectra at the former site. This in turn leads to a decreased power absorption ability of the optimally-arranged PAs in the case of S2. As for site S1, the deployment of the devices at an even smaller water depth (i.e., at d/a=3.5) combined with the existence of milder local wave climate conditions (Fig. 4a) lead to the smallest p_{annual} value among all examined sites.
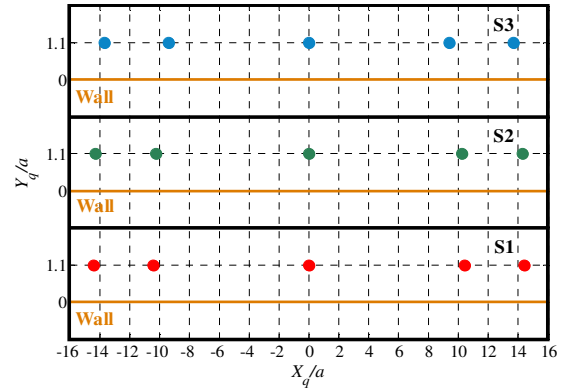
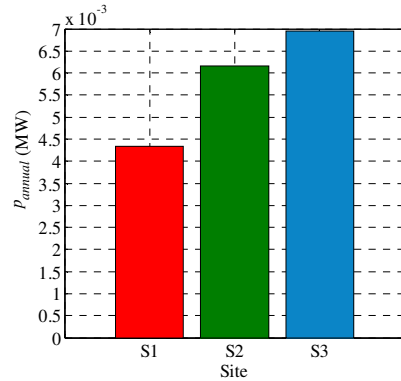Fig. 7 Optimum layouts of the PAs cluster in front of the wall for S1~S3 and for OPC2

Fig. 8 p_{annual} for S1~S3 for the optimally-arranged clusters of OPC2

Moving on to the second examined optimization case (OPC2), where the PAs are free to be situated along the whole wall length, Fig. 7 shows the corresponding optimum layouts of the PAs cluster in front of the wall in the X-Y plane, while, in Fig. 8 the maximum p_{annual} values are presented. Similarly to OPC1, the PAs of the optimum layouts for all examined sites (Fig. 7) are situated along a straight, parallel to the wall, line at the smallest allowable distance from it (i.e., at Y/a=1.1). However, contrary to OPC1, all three optimum cluster layouts are characterized by the formation of a sub-cluster of two PAs close to each wall edge. Regarding p_{annual} (Fig. 8), the largest annual power equal to 6.95 kW, is again absorbed by the optimally-arranged PAs in the case of S3, whereas for sites S2 and S1 the power absorption ability of the cluster is reduced, respectively, by 11.5% and 37.6% compared to S3. This result is similar with the corresponding one obtained in the case of OPC1 and, thus, it can be physically interpreted using the relevant discussion made above. Compared to OPC1, the distribution of

the PAs along the whole wall length, leads to an increase of the maximized p_{annual} values by 13.9%, 18.4% and 14.8% for sites S1, S2 and S3, respectively. Thus, the consideration of the whole wall length for placing the PAs, which enables the realization of a wider PAs' distribution along the leeward boundary, enhances the power absorption ability of the PAs cluster.

The effect of the action of oblique waves on the formation of the optimum cluster layouts and on the maximum p_{annual} absorbed by the cluster is demonstrated with the aim of Figs. 9~10 respectively, where the results of the third examined optimization case (OPC3) are plotted. It is reminded that in OPC3 the whole wall length is considered available for the placement of the devices, similarly to OPC2. For all three sites examined, PAq, q=1, 2, 3 and 4 of the optimum layouts (Fig. 9) are located at the smallest allowable perpendicular distance from the wall (i.e., at Y/a=1.1) as in OPC2, while the middle device (PA3) is situated slightly further from the leeward boundary (i.e., at Y_3/a=1.2 for S1 and S2 and at Y_3/a=1.95 for S3). In the case of site S1, two sub-clusters of two closely-positioned devices each are identified close to the two edges of the leeward boundary. This is not observed for site S2, where the PAs are distributed uniformly at -13.1<X/a<13.1 with a center-to-center distance equal to 6.55a. Similar is the optimum layout pattern for S3; however, for this site, PAq, q= 2 and 4 are situated closer to the corresponding outer PA.
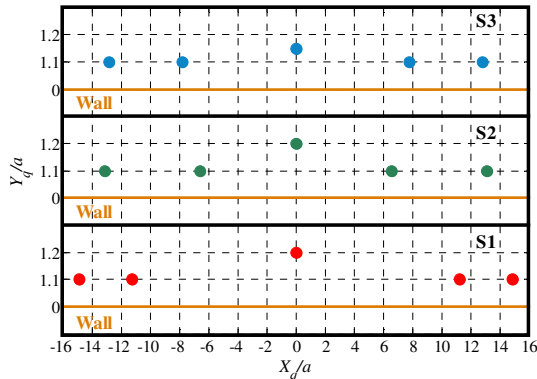

Fig. 9 Optimum layouts of the PAs cluster in front of the wall for S1-~S3 and for OPC3
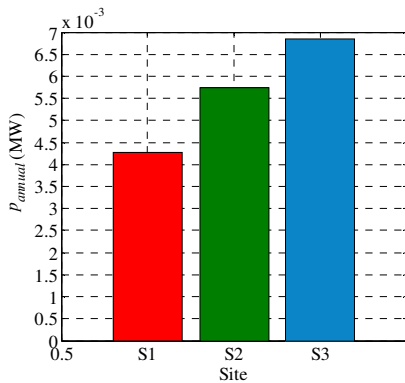

Fig. 10 p_{annual} for S1~S3 for the optimally-arranged clusters of OPC3

As for the annual power absorbed by the cluster (Fig. 10), the largest p_{annual} value equal to 6.86 kW is observed in the case of site S3, similarly to OPC1 (Fig. 6) and OPC2 (Fig. 8). For sites S2 and S1 the power absorption ability of the PAs cluster is reduced by 16.3% and 37.8%, respectively, compared to S3 for the reasons previously explained. Taking into account the results of Fig. 8, where optimum layouts are realized for perpendicular to the wall waves, the action of oblique waves leads to a small decrease of the power absorbed by the optimally-arranged cluster. More specifically, compared to OPC2, the maximized p_{annual} values are decreased by 1.7%, 6.8% and 1.4% for sites S1, S2 and S3, respectively.

CONCLUSIONS

In the present paper, we develop numerically an optimization process to determine the optimum layout of a cluster of PAs in front of a bottom-mounted vertical wall of finite length under the action of long-crested irregular waves. The term "optimum" refers to layouts that maximize the annual power absorbed by the cluster and satisfy predefined spatial constraints. The developed optimization process is applied for a cluster of five oblate spheroidal PAs deployed at three near-shore sites in the Aegean Sea, Greece. These sites are characterized by mild wave environmental conditions and sea states with T_p values larger than the heave natural period of the examined device. The main conclusions of the present investigation for the specific PAs' characteristics and for the wave climate conditions considered can be summarized as follows:

• Under the action of perpendicular to the wall waves, the optimum cluster layouts for all sites examined have the form of linear arrays, which are located parallel to the wall at the smallest allowable perpendicular distance from it. The siting of optimum layouts at the aforementioned distance can be related to the deployment of devices with heave natural period smaller than the peak periods of the most frequent sea states. When part of the available wall length is considered for the PAs' placement, an almost uniform distribution of the devices within the allowable wall length is observed or a sub-cluster of closely-positioned devices in the middle part of the wall is identified, depending upon the examined site. However, when the PAs are free to be situated along the whole wall length, a sub-cluster of two PAs close to each wall edge is formed for all sites. Thus, the placement of devices close to the wall edges seems to be crucial for maximizing the annual absorbed power, irrespectively of the site's local characteristics.

• The action of oblique to the wall waves introduces differences on the formation of the optimum cluster layouts. Specifically, pure linear arrangements are not formed, since the siting of the middle PA is realized slightly further from the leeward boundary compared to the rest devices. Furthermore, depending upon the examined site, the optimum layouts are characterized by either almost uniformly distributed devices within the wall length or by the formation of a sub-cluster of two closely-positioned devices close to each wall edge.

• For a given optimization case, the largest value of the annual power, p_{annual}, absorbed by the optimally-arranged clusters is obtained for site S3 (South-Eastern Aegean). In the case of site S2 (Central Aegean), the existence of a smaller water depth for the cluster's deployment leads to a reduction of the finite-depth spectral densities of the incident wave spectra. Accordingly, for this site, an average reduction of the power absorption ability of the corresponding optimally-arranged clusters by 14% compared to S3 is observed. As for site S1 (Central Aegean), the existence of an even smaller water depth along with milder local wave conditions lead to an average reduction of p_{annual} by 37.5% and by 27.3% compared to S3 and S2 respectively.

• Under the action of perpendicular to the wall waves, the utilization of the whole wall length for placing the PAs enhances the power absorption ability of the PAs cluster. Specifically, an average increase of p_{annual} by 15.7% is observed compared to the case, where part of the

wall length is utilized for placing the devices. The action of oblique to the wall waves has a small effect on the p_{annual} absorbed by the optimally-arranged clusters, since an average decrease of only 3.3% is realized compared to the action of perpendicular to the wall waves.

The present numerical investigation could be extended, so that an optimum number of PAs in front of the wall can be determined along with their optimum layout. Moreover, the determination of optimally-arranged PAs without taking into account symmetry constraints, as well as the inclusion of cost-related aspects in the formation of the optimization problem could present items for future investigation.

REFERENCES

Balitsky, P, Fernandez, GV, Stratigaki, V, and Troch, P (2018). "Assessment of the Power Output of a Two-Array Clustered WEC Farm Using a BEM Solver Coupling and a Wave-Propagation Model," *Energies*, 11(11), paper No. 2907.

Bergdahl, L (2009). "Comparison of Measured Shallow-water Wave Spectra with Theoretical Spectra," *Proc 8th European Wave and Tidal Energy Conf*, Uppsala.

Chatzigiannakou, MA, Dolguntseva, I, and Leijon, M (2017). "Offshore Deployments of Wave Energy Converters by Seabased Industry AB," *J Mar Sci Eng*, 5(2), paper No. 15.

Child, BFM, and Venugopal, V (2010). "Optimal Configurations of Wave Energy Device Arrays," *Ocean Eng*, 37(16), 1402-1417.

Deb, K (2001). *Multi-Objective Optimization Using Evolutionary Algorithms*, John Wiley & Sons, 518.

Det Norske – Germanischer Lloyds (DNV – GL) (2017). *Environmental Conditions and Environmental Loads*, *Recommended Practice DNV RP-C205*, Det Norske Veritas, 259.

Falnes, J, and Kurniawan, A (2020). *Ocean Waves and Oscillating Systems: Linear Interactions Including Wave-Energy Extraction, 2nd edition*, Cambridge University Press, 307.

Folley, M, Babarit, A, Child, B, Forehand, D, O'Boyle, L, Silverthorne, K, Spinneken, J, Stratigaki, V, and Troch P (2012). "A Review of Numerical Modelling of Wave Energy Converter Arrays," *Proc 31st Int Conf Ocean, Offshore and Arctic Eng*, ASME, Rio de Janeiro, paper No. 10.1115/OMAE2012-83807.

Gkaraklova, S, Chotzoglou, P, and Loukogeorgaki, E (2021). "Frequency-Based Performance Analysis of an Array of Wave Energy Converters around a Hybrid Wind–Wave Monopile Support Structure," *J Mar Sci Eng*, 9(1), paper No. 2.

Göteman, M, Giassi, M, Engström, J, and Isberg, J (2020). "Advances and Challenges in Wave Energy Park Optimization – A review," *Front Energy Res*, 8, paper No. 26.

Hansen, RH, Kramer, MM, and Vidal, E (2013). "Discrete Displacement Hydraulic Power Take-Off System for the Wavestar Wave Energy Converter," *Energies*, 6(8), 4001-4044.

Hughes, SA (1984). *The TMA Shallow-water Spectrum Description and Applications*, Technical Report CERC-84-7, Coastal Engineering Research Center, Department of the Army, US Army Corps of Engineers, 46.

Konispoliatis, DN, and Mavrakos SA (2020). "Wave Power Absorption by Arrays of Wave Energy Converters in Front of a Vertical Breakwater: A Theoretical Study," *Energies*, 13(8), paper No. 1985.

Konispoliatis, DN, Mavrakos SA, and Katsaounis, GM (2020). "Theoretical Evaluation of the Hydrodynamic Characteristics of Arrays of Vertical Axisymmetric Floaters of Arbitrary Shape in front of a Vertical Breakwater," *J Mar Sci Eng*, 8(1), paper No. 62.

Lavidas, G, Agarwal, A, and Venugopal, V (2018). "Availability and Accessibility for Offshore Operations in the Mediterranean Sea," *J Waterw Port Coast Ocean Eng*, 144(6), 1-13.

Lavidas, G, and Venugopal, V (2017). "A 35 Year High-resolution Wave Atlas for Nearshore Energy Production and Economics at the Aegean Sea," *Renew Energy*, 103, 401-417.

Lee, CH (1995). *WAMIT Theory Manual*, MIT Report 95-2, Department of Ocean Engineering, MIT, 66.

Lee, CH, and Newman, JN (2005). *Computation of Wave Effects using the Panel Method*, in Numerical Models in Numerical Models in Fluid-Structure Interaction (Chakrabarti S, editor), WIT Press, 211-251.

Loukogeorgaki, E, and Chatjigeorgiou, IK (2019). "Hydrodynamic Performance of an Array of Wave Energy Converters in Front of a Vertical Wall," *Proc 13th European Wave and Tidal Energy Conf*, Napoli, paper No. 1464.

Loukogeorgaki, E, Boufidi, I, and Chatjigeorgiou, IK (2020). "Performance of an Array of Oblate Spheroidal Heaving Wave Energy Converters in Front of a Wall," *Water*, 12(1), paper No. 188.

MATLAB (2019). *Version 9.7 (2019b)*, Natick, Massachusetts, United States: The MathWorks, Inc.

Mavrakos, SA, Katsaounis, GM, Nielsen, K, and Lemonis, G (2004). "Numerical Performance Investigation of an Array of Heaving Wave Power Converters in front of a Vertical Breakwater," *Proc 14th Int Offshore and Polar Eng Conf*, Toulon, ISOPE, 3, 1170–1178.

Michailides, C, and Angelides, DC (2015). "Optimization of a Flexible Floating Structure for Wave Energy Production and Protection Effectiveness," *Eng Struct*, 85, 249-263.

Neshat, M, Abbasnejad, E, Shi, Q, Alexander, B, and Wagner, M (2019). "Adaptive Neuro-Surrogate-Based Optimisation Method for Wave Energy Converters Placement Optimisation," *Proc Int Conf Neural Inf Process*, Sydney, 353–366.

Rosa-Santos, P, Taveira-Pinto, F, Clemente, D, Cabral, T, Fiorentin, F, Belga, F, and Morais T (2019). "Experimental Study of a Hybrid Wave Energy Converter Integrated in a Harbor Breakwater" *J Mar Sci Eng*, 7(2), paper No. 33.

Ruiz, PM, Nava, V, Topper, MBR, Minguela, PR, Ferri, F, and Kofoed, JP (2017). "Layout Optimisation of Wave Energy Converter Arrays," *Energies,* 2017, 10(9), paper No. 1262.

Rusu, E, and Onea, F (2018). "A Review of the Technologies for Wave Energy Extraction," *Clean Energy*, 2(1), 10-19.

Sarkar, D, Contal, E, Vayatis, N, and Dias, F (2016). "Prediction and Optimization of Wave Energy Converter Arrays using a Machine Learning Approach," *Renew Energy*, 97, 504-517.

Sharp, C, and DuPont, B (2018). "Wave Energy Converter Array Optimization: A Genetic Algorithm Approach and Minimum Separation DIstance Study," *Ocean Eng*, 163, 148-156.

Stratigaki, V, Troch, P, Stallard, T, Forehand, D, Kofoed, JP, Folley, M, Benoit, M, Babarit, A, and Kirkegaard, J (2014). "Wave Basin Experiments with Large Wave Energy Converter Arrays to Study Interactions between the Converters and Effects on Other Users in the Sea and the Coastal Area," *Energies*, 7(2), 701-734.

Tzellos, N, Loukogeorgaki, E, Anastasiou, E, and Chatjigeorgiou, IK (2020). "Performance of an Oblate Spheroidal Heaving Wave Energy Converter," *Proc 30th Int Offshore and Polar Eng Conf*, Shanghai, ISOPE, 1, 116–123.

Vicinanza, D, Margheritini, L, Kofoed, JP, and Buccino, M (2012). "The SSG Wave Energy Converter: Performance, Status and Recent Developments," *Energies*, 5(2), 193-226.

Zhao, XL, Ning, DZ, Zou, QP, Qiao, DS, Cai, SQ (2019). "Hybrid Floating Breakwater-WEC system: A Review," *Ocean Eng*, 186, paper No. 106126.

\Conf-std\Template-Word-MS-2021bott